# Chemical and magnetic phase diagrams of $AB_3$ and $A_3B$ anisotropic thin films

H. O. Gonzalez Ochoa and F. Aguilera-Granja
*Instituto de Fisica, Universidad Autonoma de San Luis Potosi, Alvaro Obregon 64, 78000 San Luis Potosi, SLP, Mexico*

V. Pierron-Bohnes and M. C. Cadeville
*Institut de Physique et de Chimie des Matériaux de Strasbourg (IPCMS), Groupe d'Etude des Matériaux Métalliques (GEMM), UM0046 CNRS-ULP-ECPM, 23 rue du Loess, F-67037 Strasbourg, France*
(Received 17 May 1999; revised manuscript received 7 April 2000)

We present a double Ising model treated in the Bragg-Williams approximation with aim to describe the composition modulations and the magnetic properties of MBE codeposited fcc (111) oriented alloy thin films. First the chemical and magnetic phase diagrams of isotropic $AB_3$ and $A_3B$ fcc structures with $A$ the magnetic component are calculated. Then the effect of anisotropic chemical interactions that are different in the basic (111) planes and between these planes is investigated. It yields the formation of a superlattice-like system analogous to those experimentally observed in some Co-based alloy films. On the $B$-rich side, the magnetic phase diagrams are strongly modified with respect to the isotropic case. Comparison is made with experimental data.

## I. INTRODUCTION

Recent investigations of hcp and fcc Co-based MBE coevaporated thin films (Co-Ru, Co-Pt), grown in the hexagonal [0001] or [111] plane, have shown the presence of a composition modulation along the growth direction with an amplitude which is strongly dependent on the growth temperature and the alloy composition. Such a modulation, we name anisotropic long range order (ALRO), does not exist in the corresponding equilibrium bulk phase diagrams. The Co-Ru equilibrium bulk phase diagram displays a complete hcp solid solution over the whole concentration range at low temperature[1] whereas the Co-Pt equilibrium bulk phase diagram presents $L1_2$, $L1_0$, and $L1_2$ structures ordered on the fcc lattice for respectively the $A_3B$, $AB$, and $AB_3$ compositions.[2] This ALRO has been observed in hcp $Co_{1-x}Ru_x$ alloys[3,4] over the whole explored concentration range ($0.05 \leqslant x \leqslant 0.95$) and in hcp and fcc $Co_{1-x}Pt_x$ on the Co-rich side[5–7] and with a very weak intensity in fcc $Co_{50}Pt_{50}$.[6] LRO was never observed in the hexagonal growth plane. On the Pt-rich side of [111] Co-Pt films ($x \sim 0.75$) one does not observe a composition modulation, but a strong enhanced perpendicular magnetic anisotropy[7–9] and anomalous high values of the Curie temperatures.[8] Perpendicular magnetic anisotropy was assigned to the presence of an anisotropic chemical short range order[10] (ASRO) whereas the high values of the Curie temperatures have been explained by Ref. 8 in terms of the presence of a miscibility gap at low temperatures, that could be either an equilibrium state not yet observed in bulk alloys for lack of diffusion, or a metastable phase separation driven by surface magnetic interaction effects. Some structural and magnetic properties of these thin films are summarized in Fig. 1. As illustrated, all properties display the same kind of dependence with the growth temperature but the concentration dependence of the ALRO measured at the optimal growth temperature is typical of each system.

Both LRO and ASRO were presumed by Ref. 11 to have qualitatively the same physical origin. They are qualitatively described in terms of a double competition between surface and bulk diffusion, and surface and bulk interactions. The surface interactions produce preferential occupation of the surface plane by one of the two components (surface segregation effect) at the detriment of the underlying plane, leading to alloy thin films that could be seen as surface alloys stacked above each other bilayer by bilayer and progressively frozen-in as the free surface is advancing.

To observe this metastable alloy, the surface diffusion compared to the deposition rate of a bilayer must be high enough to allow the surface atomic equilibrium rearrangement to take place during the growth time and the bulk diffusion low enough to prevent from the diffusion in buried

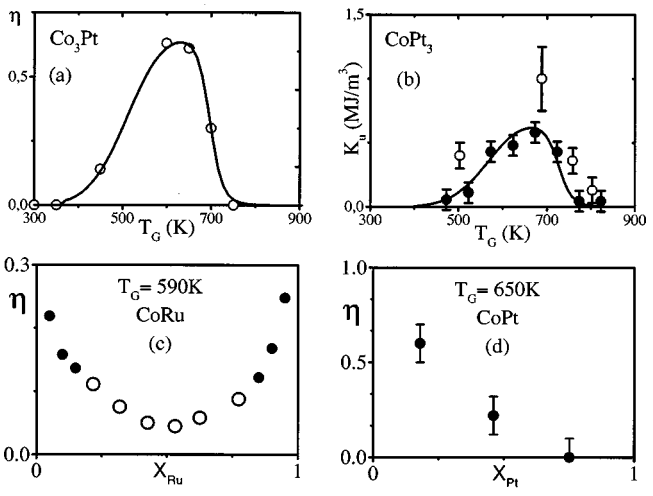


FIG. 1. Experimental results: temperature dependence of long range order in $Co_3Pt$ [(a) ○ (Ref. 5)] and magnetic anisotropy in $CoPt_3$ [(b) ● (Ref. 8) and ○ (Ref. 9)] and their simulation in a thermoactivated model (Ref. 11) (full lines), concentration dependence of long range order in Co-Ru (Ref. 4) [the results of two different series (● and ○) are normalized] (c), and Co-Pt (Ref. 6) (d).

 

layers that would tend to restore the bulk equilibrium thermodynamic state. A thermoactivated model that takes into account both surface and bulk effects describes the temperature dependence of observed structural and magnetic properties (Fig. 1).[11]

In order to describe the properties of the anisotropic systems built in this way and to get a rough estimate of the role played by the presence of anisotropic chemical interactions (superlattice like system), we have developed a simple model (Bragg-Williams approximation) to calculate phase diagrams in presence of chemical and magnetic interactions, focusing on systems with a fcc structure. This model, presented in Sec. II, is presumed to represent the Co-Pt system which is magnetic over the whole composition range, treating the $A_3B$ (Co-rich side) and $AB_3$ (Pt-rich side) compositions, $A$ being the magnetic component. The results are given in Sec. III. First we present the results obtained in the case of an isotropic bulk system, illustrating the effect of the hierarchy between first nearest neighbor chemical interactions and first and second nearest neighbor magnetic interactions. Then we calculate the phase diagrams in presence of anisotropic chemical interactions along the [111] direction that induce composition modulations between adjacent planes, in order to reproduce those observed in alloy thin films. Section IV is devoted to the discussion and conclusions.

## II. MODEL

We consider two binary alloys $A_{1-x}B_x$ with one magnetic component ($A$) and $x=0.25$ and $x=0.75$ in a fcc structure which are ordered in the $L1_2$ structure at low temperature. With the aim of studying the different ordered phases, the fcc lattice is subdivided into two interpenetrating nonequivalent sublattices $\alpha$ and $\beta$, such that the number of $\alpha$ and $\beta$ sites are respectively 1/4 and 3/4 of the total number of sites in the system. The $\alpha$ sites have twelve $\beta$ sites as first nearest neighbors, and the $\beta$ sites have four $\alpha$ and eight $\beta$ sites as first nearest neighbors and the $\alpha$ ($\beta$) sites have six $\alpha$ ($\beta$) sites as second nearest neighbors. In the ordered state the minority atoms ($B$ for $x=0.25$ and $A$ for $x=0.75$) are placed in the $\alpha$ sublattice, whereas the majority atoms are placed in the $\beta$ sublattice. Therefore no first nearest neighbor $A$-$A$ pairs are present in the spatially ordered $AB_3$ alloy, that will have drastic consequences on the interplay between chemical and magnetic orderings, comparing with the $A_3B$ phase. We study the effects of chemical and magnetic interactions on chemical and magnetic phase diagrams, within the Bragg-Williams approximation. For the chemical interactions, we consider two cases: the bulklike system (isotropic system) and the superlattice-like system (anisotropic system).

To describe the different ordered states of the system the probabilities to have a $I$ atom with a $m$ spin state ($m=\uparrow,\downarrow$) in the $\nu$ sublattice are noted by $P_\nu^{Im}$. Only first nearest neighbor interactions are considered for the chemical contribution as it is sufficient to get the ordered $L1_2$ equilibrium state. Expressions are given for the $AB_3$ case.

The chemical energy in terms of the probabilities is given by

$$U_C=-3NU[(P_\alpha^{A\uparrow}+P_\alpha^{A\downarrow})P_\beta^B+(P_\beta^{A\uparrow}+P_\beta^{A\downarrow})(P_\alpha^B+2P_\beta^B)],$$

where $N$ is the total number of lattice sites, $-U$ is the energy needed to form an $A$-$B$ pair. $U_{AA}$ and $U_{BB}$, the energies needed to form the $A$-$A$ and $B$-$B$ pairs, have been taken equal to zero for the sake of simplicity without lost of generality.

For the magnetic energy, we consider first and second nearest neighbor ferromagnetic interactions, the magnetic contribution is written as

$$U_M=-3NJ_1[(P_\alpha^{A\uparrow}-P_\alpha^{A\downarrow})(P_\beta^{A\uparrow}-P_\beta^{A\downarrow})+(P_\beta^{A\uparrow}-P_\beta^{A\downarrow})^2]$$
$$-\frac{3}{4}NJ_2(P_\alpha^{A\uparrow}-P_\alpha^{A\downarrow})^2-\frac{9}{4}NJ_2(P_\beta^{A\uparrow}-P_\beta^{A\downarrow})^2,$$

where $-J_1$ and $-J_2$ are the energies associated with first and second neighbor pairs of parallel spins, respectively. The total internal energy is $U=U_C+U_M$.

The entropy is given by the Boltzmann equation $S=-k_B\ln\Omega$, where $\Omega$ is the number of different configurations. To get the equilibrium state of the system, the free energy ($F=U-TS$) is minimized with respect to the probabilities. Additional conditions such as concentration and normalization have to be included in the minimization. Thus, at each temperature, the probabilities are deduced from a matrix inversion.

Two types of order parameters are defined to study the system, one chemical and two magnetic parameters. The spatial order parameter is defined as

$$\eta=(P_\alpha^{A\uparrow}+P_\alpha^{A\downarrow})-(P_\beta^{A\uparrow}+P_\beta^{A\downarrow}),$$

and the magnetic order parameter for each sublattice is defined as

$$m_\nu=(P_\nu^{A\uparrow}-P_\nu^{A\downarrow}),\quad \nu=\alpha,\beta.$$

The order-disorder transition temperature ($T_{OD}$) and the Curie temperature ($T_{CM}$) correspond to the cancelling of the respective order parameters.

In the anisotropic case, the model corresponds to a superlattice with a basic unit of two (111) parallel planes (Fig. 2). This anisotropy should roughly mimic the difference between the chemical interactions inside the surface and the subsurface planes. We define different interaction energies inside the $[k]$ and $[k+1]$ planes with an anisotropy ratio $R_A=U_k/U_{k+1}$ and $W=U$ between the two planes. Different anisotropy ratios will be considered.

## III. RESULTS

### A. Isotropic case

The shapes of chemical and magnetic phase diagrams have been explored over a very broad range of magnetic ($J_1$, $J_2$) and chemical ($U$) interaction parameters. The detailed results are presented in Master degree thesis of Gonzalez Ochoa.[13] Here we focus on results that are as close as possible of the Co-Pt system on both concentration sides, being aware of the oversimplification of the model which assumes concentration independent $J$ and $U$ parameters.[12] In all calculated cases, as expected, the chemical O-D transition is of first order whereas the magnetic transition is of second order. When both transition temperatures are superimposed, the

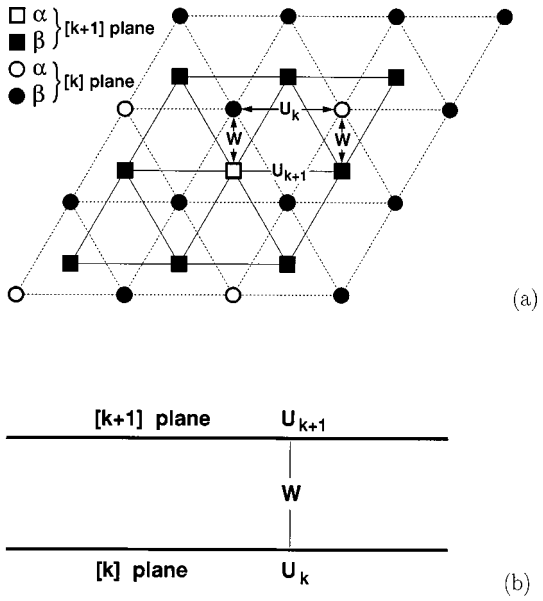


FIG. 2. Illustration of the model used in this work for the superlattice-like systems with basic unit of two parallel planes. The value of the chemical interactions are $U_k$ for the $[k]$ plane, $U_{k+1}$ for the $[k+1]$ plane and $W$ for the interplanar interaction.

transition is of first order. In Fig. 3, we present the $AB_3$ phase diagram for $k_BT/U$ vs $J_1/U$ with $J_2=0$ [Fig. 3(a)] and $J_2=0.15\,U$ [Fig. 3(b)]. As expected, a nonzero $J_2$ interaction is necessary to introduce magnetic order in the ordered state. In Fig. 3(b), for $J_1<0.55\,U$ there still exists a

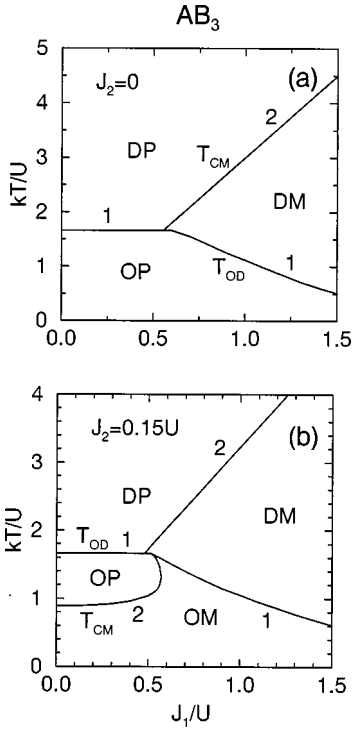


FIG. 3. Phase diagram of isotropic $AB_3$ system for $k_BT/U$ vs $J_1/U$ with $J_2=0$ (a) and $J_2=0.15\,U$ (b). The transition order (first or second order) are indicated by the numbers in the figures. The state of the alloy in the different ranges are indicated by capital letters: chemically ordered (O) or disordered (D), and magnetically ordered (M) or paramagnetic (P).

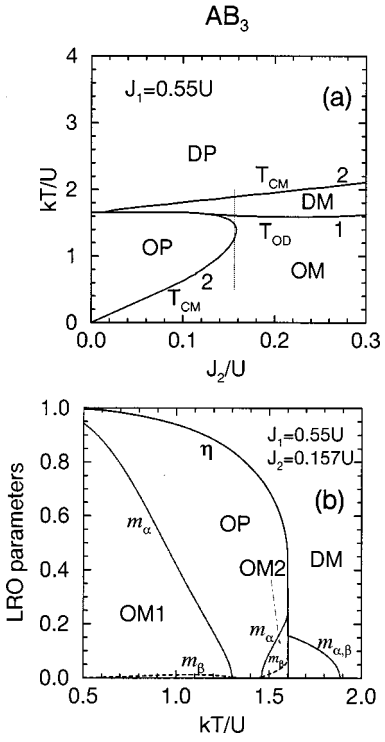


FIG. 4. (a) Phase diagram for isotropic $AB_3$ system for $k_BT/U$ vs $J_2/U$ with $J_1=0.55\,U$. (b) Long range order parameters as a function of the temperature for $J_1=0.55\,U$ and $J_2=0.157\,U$, as indicated by the vertical line in (a). Notice the presence of two Curie temperatures.

paramagnetic phase in the order state: the Curie temperature ($T_{CM}$) is lower than the order-disorder transition ($T_{OD}$). This situation corresponds to the $CoPt_3$ case[14] for which the value of the experimental ($T_{CM}/T_{OD}$) ratio is 0.3. It would be possible to stay closer of the experimental value by decreasing $J_2$, but without physical interest, on account of the approximations of the model. When increasing $J_2$ the OP (ordered paramagnetic) region of Fig. 3(a) disappears at the detriment of the OM (ordered magnetic) region. The $J_2$ dependence of the phase diagrams for a peculiar value of $J_1$ is shown in Fig. 4(a). It illustrates both the strong sensitivity of $T_{CM}$ with $J_2$ and the possibility that the magnetism reappears at high temperature in the disordered state. As an example of a given alloy system, the temperature dependence of the order parameters is presented in Fig. 4(b), for $J_1=0.55\,U$ and $J_2=0.157\,U$, illustrating a system that shows two Curie temperatures, a low Curie temperature for the ordered state and a high Curie temperature for the disordered state. It is worth to notice that the magnetic order reappears with a spatial order similar to the order present at low temperature; although both of them are equal, we call it OM2 to differentiate it from the OM1 that corresponds to the low temperature order state.

Figures 5(a) and 5(b) are the equivalents of Figs. 3(a) and 3(b) in $A_3B$. The effect of $J_2$ is obviously less important than in $AB_3$ and for $J_1 \geqslant 0.1\,U$ or $0.2\,U$, depending on $J_2$, $T_{CM}$ is higher than $T_{OD}$. The couple of values $J_2=0.15\,U$ and $J_1$ between 0.2 and $0.3\,U$ corresponds to the experimental ratio $T_{CM}/T_{OD}=1.4$ in $Co_3Pt$.[14] This couple of $J_1$ and $J_2$ values is also convenient to describe $CoPt_3$ as seen in the previous section.

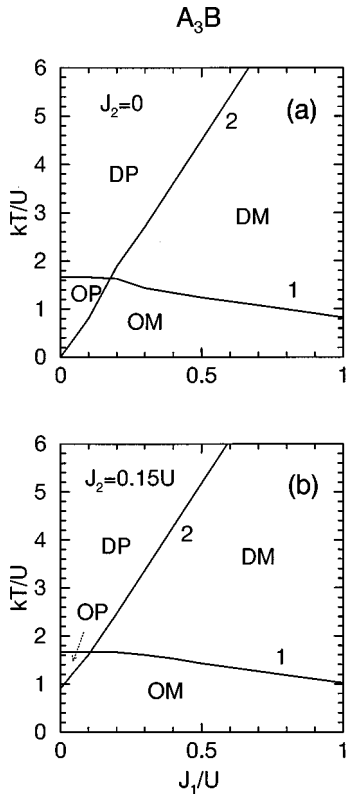


FIG. 5. Phase diagram of isotropic $A_3B$ system for $k_BT/U$ vs $J_1/U$ with $J_2=0$ (a) and $J_2=0.15\,U$ (b).

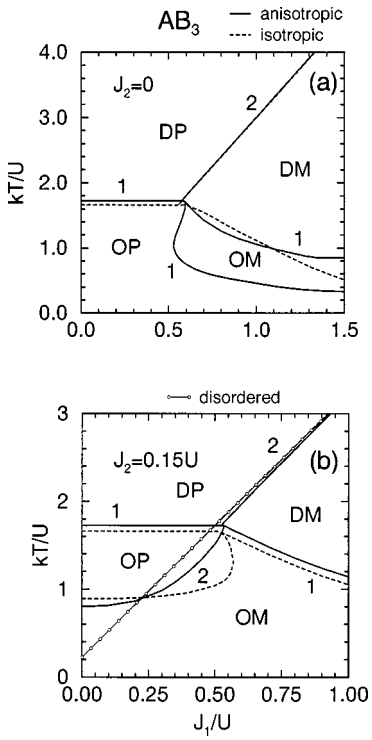


FIG. 6. Phase diagram in $AB_3$ system for $k_BT/U$ vs $J_1/U$ with $J_2=0$ (a) and $J_2=0.15\,U$ (b), for isotropic (dashed line) and anisotropic (full line, $R_A=3$) cases, the circles correspond to the disordered alloy. In the anisotropic case with $J_2=0$ (a), the OM phase appears as a consequence of the concentration modulation.

To summarize, our model shows that, for the isotropic case, one can find a unique set of parameters than reproduces the orders of magnitude of the Curie and order-disorder temperatures on both sides of the Co-Pt phase diagram. As far as $J_1$ and $J_2$ are smaller than $U$, the presence of magnetism slightly influences the chemical phase diagram, but the degree of chemical disorder and the relative values of $J_1$ and $J_2$ strongly modify the magnetic phase diagram especially on the $AB_3$ side.

### B. Anisotropic case

We have chosen to treat in detail both systems with a high anisotropy ratio: $R_A=U_k/U_{k+1}=3$ with $U_k=1.5\,U$ for the $[k]$ plane, and $U_{k+1}=0.5\,U$ in the $[k+1]$ plane and $W=U$ between the two planes. A case with a small anisotropy ($R_A=1.22$) is treated for the $AB_3$ composition only.

#### *1. $AB_3$ composition*

The anisotropic cases ($R_A=3$) of the phase diagrams presented in Figs. 3(a) and 3(b) are shown in Figs. 6(a) and 6(b). For $J_2=0$ [Fig. 6(a)] an important difference lies in the appearance of magnetic ordering (OM phase) in the chemically ordered phase. This OM phase appears as a consequence of the modulation in concentration of the magnetic component, that induces the formation of first nearest neighbor $A$-$A$ pairs not present in the isotropic case at low $T$. For $J_2=0.15$ [Fig. 6(b)], the Curie temperatures of a quenched disordered state are also shown for comparison. In the anisotropic case, the Curie temperature of the ASRO phase quenched from high temperature is also the prolongation of the high temperature straight line (not shown in the figure). For the set of $J_1/U$ values we are interested in, i.e., around 0.3, the Curie temperatures of the anisotropic case are clearly higher than those of the isotropic case, but remain lower than those of the quenched disordered state. Let us note that the experimental ratio of 1.4 between the Curie temperatures in the quenched disordered bulk $CoPt_3$ phase and in the $L1_2$ ordered phase[14] is also well reproduced by the same set of $J_1$ ($0.3\,U$ $-0.35\,U$) and $J_2$ ($0.15\,U$) parameters. The $kT/U$ dependence of LRO parameters and concentrations in respectively $[k]$ and $[k+1]$ planes for these $J_1$ and $J_2$ values are shown in Figs. 7(b),7(c) and 7(d),7(e), for two different anisotropy ratios, respectively 3 and 1.22. Figure 7(a) shows the isotropic case for comparison. As expected, a concentration modulation is actually observed, giving rise to different average concentrations $c$ in the $[k]$ and $[k+1]$ planes. The anisotropic long range order parameter ($\eta_A$), given by $(c_k-c_{k+1})/2x$, which is experimentally determined in the alloy films (Fig. 1) is also represented in Figs. 7(b) and 7(d). It increases with the disorder in the $L1_2$ region and decreases slowly with the temperature in the disordered state, disappearing at temperatures quite higher than the O-D transition.

#### *2. $A_3B$ composition*

Figure 8 compares the anisotropic case ($R_A=3$) to the isotropic case [Fig. 5(b)]. The effect of a large anisotropy on both Curie and order-disorder transitions is very small. Figure 9 shows the $kT/U$ dependence of order parameters for a given set of $J_1$ and $J_2$ values that shows the persistence of anisotropic long range order quite above the O-D transition.

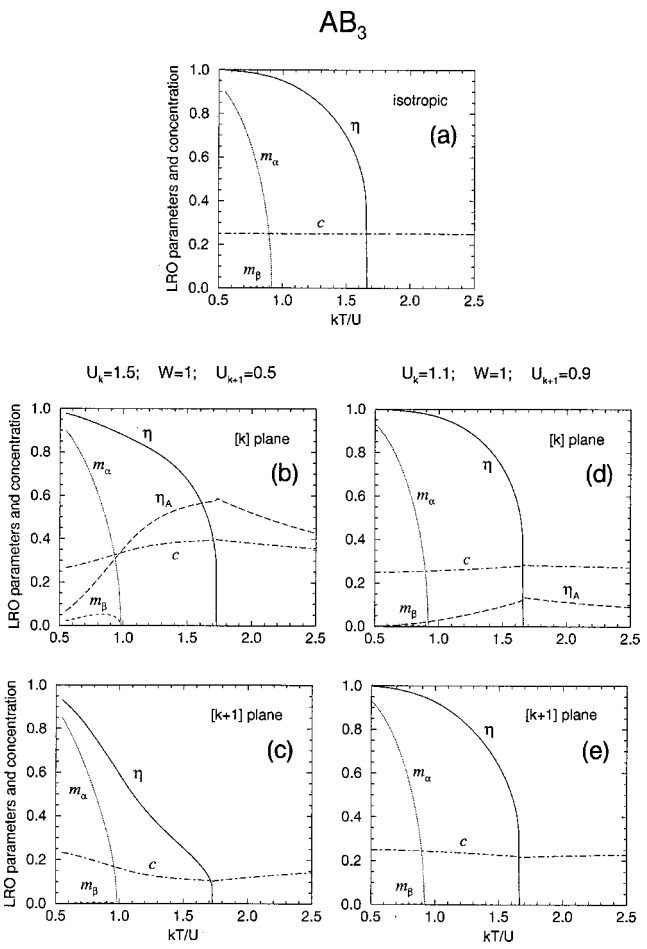


FIG. 7. Order parameters as a function of the temperature for the isotropic (a) and anisotropic (b)–(e) $AB_3$ system with $J_1=0.3\,U$ and $J_2=0.15\,U$. The $[k]$ plane is shown in (b),(d) and the $[k+1]$ plane in (c),(e) for two values of $R_A=U_k/U_{k+1}$: $R_A=3$ (b),(c) and $R_A=1.22$ (d),(e) and the ALRO parameter $\eta_A=(c_k-c_{k+1})/2x$ is plotted in (b),(d).

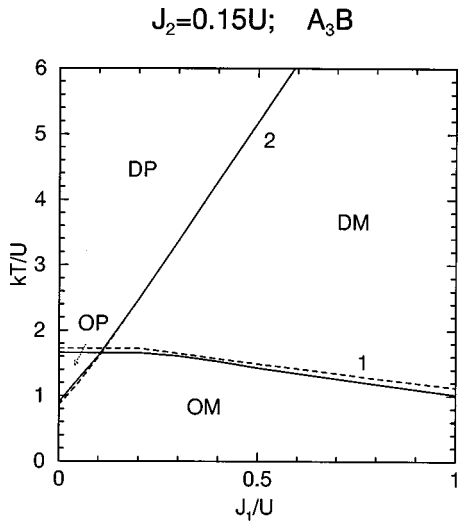


FIG. 8. Phase diagram for the isotropic (dashed line) and anisotropic (full line) $A_3B$ system for $k_BT/U$ vs $J_1/U$ with $J_2=0.15\,U$ and $R_A=3$.

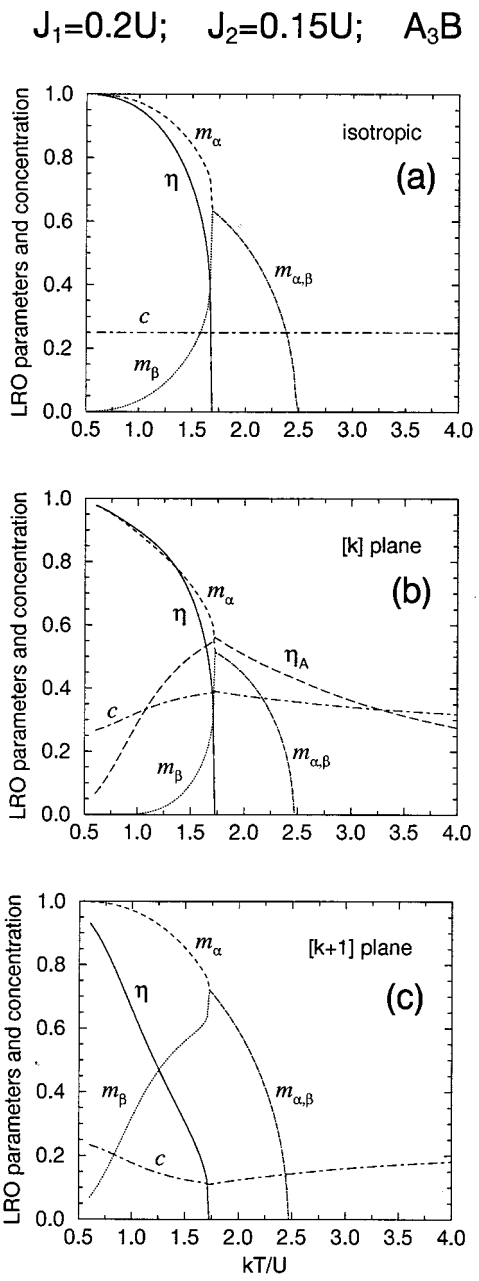


FIG. 9. Order parameters as a function of the temperature for the isotropic (a) and anisotropic (b),(c) $A_3B$ system with $J_1=0.2\,U$ and $J_2=0.15\,U$. The $[k]$ plane is shown in (b) and the $[k+1]$ plane in (c) for $R_A=U_k/U_{k+1}=3$ and the ALRO parameter $\eta_A=(c_k-c_{k+1})/2x$ is plotted in (b).

## IV. DISCUSSION AND CONCLUSION

Introducing anisotropic chemical interactions induces new interesting features in both chemical and magnetic phase diagrams as the observed composition modulation correlated to the anisotropic LRO parameter ($\eta_A$). In both $AB_3$ and $A_3B$ phases, we observe similar effects of the anisotropy and a competition between $L1_2$ ordering and anisotropic order [Figs. 7(b) and 9(b)]: ordering of the $L1_2$ structure destroys the anisotropic order which is maximum at the O-D transition and decreases slowly with temperature at high temperature. The effect of the chemical anisotropy on the magnetic properties is mainly visible on the Pt-rich side and enlarges the OM range.

Comparing with experimental results in thin films, the maximum value of $\eta_A$ close to 0.6 measured at a growth temperature of about 600 K in $Co_3Pt$ [Fig. 1(a)] is in agreement with the results of the simulation for the set of parameters of Fig. 9 ($R_A=3$). The situation is different in $CoPt_3$. Experimentally, no composition modulation has been found, only ASRO is observed, whereas the simulation data display large values of $\eta_A$ as in $Co_3Pt$. A quite smaller value of the anisotropy ratio should be introduced to get nonobservable values of $\eta_A$ [Fig. 7(d)].

Surface segregation is presumed to be at the origin of the composition modulations in these Co-Pt films. Surface segregation measurements on (111) surfaces of Co-Pt alloys[15] have shown a strong Pt enrichment of the superficial plane and a Co enrichment in the underlying plane; the Pt concentrations are respectively 0.46 and 0.03 in $Co_3Pt$ and of 1 and 0.48 in $Co_{20}Pt_{80}$. That would lead to $\eta_A$ values close to their maximum value of 1. The reason why ASRO instead of composition modulations was observed until now in $CoPt_3$ films is thus not clear since surface segregation trends are comparable on both sides of the Co-Pt phase diagram. Nevertheless, as probed by polarized XAFS,[10] the presence of preferential Co-Pt pairs out of the (111) plane balanced by preferential Co-Co pairs in the film plane is also in favor of local concentration differences between two adjacent planes, but their planar coherency would be too small to give rise to a superstructure line.

This different behavior in $Co_3Pt$ and $CoPt_3$ films could be originated by their different structure, respectively hcp and fcc. Whereas a bilayer by bilayer growth mode, that originates the composition modulations as proposed by Ref. 4 would be favored by a *ABAB* stacking of (0001) planes in a hcp structure, it would be less favored by the *ABC* stacking of a fcc structure. As a matter of fact, in Co-Ru alloy thin films that have a hcp structure over the whole concentration range, and that we do not intend to model here, an anisotropic LRO parameter is observed over the whole composition range, with smaller values of $\eta_A$ (0–0.4) [Fig. 1(c)].

Another result of this model lies in the effect of the chemical anisotropy on the magnetic properties. As seen, this effect is important on the Pt-rich side. The magnetic properties of $CoPt_3$ films investigated by Rooney *et al.*,[8] as mentioned in the introduction, are characterized by Curie temperatures that are much higher than those of the disordered state. In our model, for the set of parameters that describe $CoPt_3$ (Fig. 6) the presence of a chemical anisotropy increases the Curie temperatures with respect to the isotropic phase, but $T_{CM}$ stay smaller than in the quenched disordered state: even when changing the ratio $J_2/U$ and when increasing the anisotropy ratio, our model does not reproduce Curie temperatures superior to those of the disordered state. The high values of $T_{CM}$ experimentally observed in $CoPt_3$ films would correspond to a strong local order (clustering Co atoms) that cannot be described by our model.

To conclude, the simple model we have developed to calculate chemical and magnetic phase diagrams of anisotropic $A_3B$ and $AB_3$ thin films is able to describe the presence of composition modulations as in built thin films. The absence of ALRO in $CoPt_3$ films can have a structural origin. Moreover when magnetic interactions are clearly smaller than chemical interactions, i.e., when the magnetic order is less stable than the chemical order, the magnetic properties are very sensitive to the degree of chemical order, that induces a great variety of situations for the magnetic phases. Over a broad range of interaction parameters, the Curie temperature in $AB_3$ anisotropic films are higher than in $L1_2$ ordered isotropic films, but always lower than in the disordered phase. A model that takes into account the pair correlations (Bethe or higher order approximation of the cluster variation method) has still to be built to treat more precisely the magnetic properties of these thin films. The case of hcp films will be treated in the near future.

## ACKNOWLEDGMENT

This work has been partially supported by CONACyT, Mexico, Grant No. 25851-E.

[1] M. Hansen and K. Anderko, *Constitution of Binary Alloys* (McGraw-Hill, New York, 1958).

[2] J. M. Sanchez, J. L. Moran-Lopez, C. Leroux, and M. C. Cadeville, J. Phys.: Condens. Matter **1**, 491 (1988).

[3] L. Bouzidi, V. Pierron-Bohnes, O. Haemmerlé, C. Bouillet-Ulhaq, and M. C. Cadeville, Thin Solid Films **318**, 215 (1998).

[4] O. Ersen, L. Bouzidi, V. Pierron-Bohnes, and M. C. Cadeville, in *Mechanisms and Principles of Epitaxial Growth in Metallic Systems*, edited by L. T. Wille, C. P. Burmester, K. Terakura, G. Comsa, and E. D. Williams, MRS Symposia Proceedings No. 528 (Materials Research Society, Pittsburgh, 1998), p. 11; and (private communication).

[5] G. R. Harp, D. Weller, T. A. Rabedeau, R. F. C. Farrow, and M. F. Toney, Phys. Rev. Lett. **71**, 2493 (1993).

[6] M. Maret, M. C. Cadeville, A. Herr, R. Poinsot, E. Beaurepaire, S. Lefebvre, and M. Bessière, J. Magn. Magn. Mater. **191**, 61 (1999).

[7] M. Maret, C. Ulhaq-Bouillet, W. Staiger, M. C. Cadeville, S. Lefebvre, and M. Bessière, Thin Solid Films **319**, 191 (1998).

[8] P. W. Rooney, A. L. Shapiro, M. Q. Tran, and F. Hellman, Phys. Rev. Lett. **75**, 1843 (1995).

[9] M. Maret, M. C. Cadeville, R. Poinsot, A. Herr, E. Beaurepaire, and C. Monier, J. Magn. Magn. Mater. **166**, 45 (1997).

[10] C. Meneghini, M. Maret, M. C. Cadeville, and J. L. Hazemann, J. Phys. IV **10**, C2-1115 (1997); C. Meneghini, M. Maret, V. Parasote, M. C. Cadeville, J. L. Hazemann, R. Cortes, and S. Colonna, Eur. Phys. J. B **7**, 347 (1999).

[11] V. Pierron-Bohnes, M. Maret, L. Bouzidi, and M. C. Cadeville, in *Diffusion Mechanisms in Crystalline Materials*, edited by Y. Mishin, N. F. B. Cowern, C. R. A. Catlow, D. Farkas, and G. Vogl, MRS Symposia Proceedings No. 527 (Materials Research Society, Pittsburgh, 1998), p. 279.

[12] E. Kentzinger, V. Parasote, V. Pierron-Bohnes, J. F. Lami, M. C. Cadeville, J. M. Sanchez, R. Caudron, and B. Beuneu, Phys. Rev. B **61**, 14 975 (2000).

[13] Gonzalez Ochoa, Master degree thesis, San Luis Potosi University, Mexico, 1999.

[14] M. C. Cadeville, C. E. Dahmani, and F. Kern, J. Magn. Magn. Mater. **54-57**, 1055 (1986).

[15] Y. Gauthier, Surf. Rev. Lett. **3**, 1663 (1996), and references therein.